Ozone-induced Acute Tracheobronchial Epithelial Injury: Relationship to Granulocyte Emigration in the Lung

Dallas M. Hyde, Walter C. Hubbard, Viviana Wong, Reen Wu, Kent Pinkerton, and Charles G. Plopper

California Primate Research Center and Department of Veterinary Anatomy and Cell Biology, School of Veterinary Medicine, University of California, Davis, California, and Division of Clinical Immunology, JHMI Asthma and Allergy Center, Baltimore, Maryland

To investigate the relationship between granulocyte emigration and epithelial injury in specific airway generations of the tracheobronchial tree following short-term ozone exposure, we exposed rhesus monkeys for 8 h to 0.00 (controls) or 0.96 ppm ozone with post-exposure periods of 1, 12, 24, 72, and 168 h in filtered air before necropsy. There were five control and three exposed monkeys for each of the post-exposure times for a total of 20 monkeys. Neutrophils isolated from peripheral blood and labeled with ^{111}In-tropolonate were infused in the cephalic vein in unanesthetized monkeys (except the 1-h group) 4 to 5 h before necropsy. The trachea and microdissected bronchi (fourth and ninth generations) and respiratory bronchioles (fifteenth generation) from the right upper lobe of each monkey were examined by electron microscopy. Labeled neutrophil influx into lung tissue and bronchoalveolar lavage fluid (BALF) was maximal at 12 h and returned to baseline by 24 h after exposure. This was in contrast to total neutrophils (labeled and unlabeled) in BALF, which were significantly elevated through 24 h after exposure but returned to baseline by 72 h. Lavage protein was significantly elevated at 24 h after exposure but was at control levels at all other times. Morphometric observations showed epithelial necrosis at 1 and 12 h in the trachea and bronchioles but continued to be observed in significant numbers at 24 h after exposure in bronchi. A significant increase in the labeling index of epithelial cells was observed at 12 h only in bronchi. Epithelial necrosis and repair was associated with the presence of granulocytes in the epithelium and interstitium of all airway levels. However, eosinophils were maximally increased in the epithelium and interstitium of bronchi at 24 h after exposure when epithelial necrosis was maximal in these airways and when lavage protein was significantly elevated. This study provides four novel observations in the evaluation of acute ozone-induced lung injury: (*1*) the sequence of epithelial injury and repair differed by airway generation, occurring earlier in the trachea and bronchioles than in bronchi; (*2*) there was a strong relationship between epithelial necrosis and the emigration and retention of neutrophils at all levels of the tracheobronchial tree; (*3*) there was a strong association between maximal epithelial necrosis, BALF protein levels, and granulocytes (especially eosinophils) in bronchi, but not the trachea and bronchioles; and (*4*) there was a strong relationship between increased mucin in BALF and loss of mucous granules in goblet cells of the tracheobronchial epithelium. We interpret these results as evidence for the contribution of granulocytes to injury and repair of the tracheobronchial epithelium after short-term ozone inhalation.

(Received in original form March 16, 1989 and in final form October 23, 1991)

Address correspondence to: Dallas M. Hyde, Ph.D., University of California, School of Veterinary Medicine, Department of Veterinary Anatomy and Cell Biology, Davis, CA 95616.

Abbreviations: adult respiratory distress syndrome, ARDS; bronchoalveolar lavage fluid, BALF; eosinophil cationic protein, ECB; enzyme-linked immunosorbent assay, ELISA; granulocyte/macrophage colony-stimulating factor, GM-CSF; high performance liquid chromatography, HPLC; lactate dehydrogenase, LDH; lipopolysaccharide, LPS; major basic protein, MBP; myeloperoxidase, MPO; prostaglandin, PG; phorbol myristate acetate, PMA; phosphate-buffered saline containing 0.05% Tween® 20, TPBS; thromboxane B_2, TXB_2.

Am. J. Respir. Cell Mol. Biol. Vol. 6. pp. 481–497, 1992

Ozone is a major constituent of photochemical smog and is known to occur at maximal concentrations of 0.5 ppm in highly polluted areas of the United States (1). It is a major health concern in these areas because of the potential toxic effects related to its oxidation properties. Oxidation of intracellular components (polyunsaturated fatty acids, sulfhydryl, or amine groups on proteins) leads to inactivation of enzymes and alterations in the structure and function of cell membranes. The respiratory system is the primary target of ozone toxicity (2).

No comprehensive study has examined the relationship between epithelial necrosis and granulocyte traffic within

the tracheobronchial tree, in bronchoalveolar lavage fluid (BALF) in acute ozone-induced lung injury, and at nonedemagenic doses of ozone. Necrosis of type I epithelial cells in proximal alveoli and of ciliated cells in bronchioles in rats exposed to ozone occurs as early as 2 h after initiation of exposure, but reaches a maximal extent by 24 h of continuous exposure by subjective evaluation (3). Exposure to 4 h of ozone followed by 20 h of exposure to filtered air, however, results in a lesion that is similar to continuous exposure by subjective evaluation (3). Epithelial necrosis in respiratory bronchioles of monkeys occurs as early as 4 h and is maximal between 12 and 24 h after the initiation of ozone exposure (4). Rabbits exposed to edemagenic doses of ozone (5 ppm) for 3 h and lavaged immediately and at 3, 6, 9, and 24 h after exposure showed an increase in granulocytes that peaked at 6 h after exposure and slowly declined thereafter (5). Similarly, rats exposed to an edemagenic dose of ozone (1.8 ppm) for 4 h followed by 24 h in filtered air showed significant increases in neutrophils, albumin, and lactate dehydrogenase (LDH) activity in BALF in the 24-h post-exposure group, but only LDH activity was significantly increased immediately after 4 h of ozone exposure (6). Lung pathology showed that lesions were restricted to the central acinus. Immediately after exposure, neutrophils were observed perivascularly within bronchiolar walls and subadjacent to the basal lamina of the bronchiolar epithelium. At 24 h after exposure, there was necrosis and attenuation of the bronchiolar epithelium with intraluminal cellular debris. It appears that the ozone-induced epithelial injury is biphasic, with an initial necrotic phase caused by direct ozone injury and a secondary phase progressing to about 24 h that is associated with a predominantly neutrophilic inflammatory infiltrate (3, 4, 6). The precise nature of this biphasic epithelial injury has not been thoroughly investigated, and no study has carefully examined the role of granulocyte traffic in the lung specifically in relationship to tracheobronchial injury resulting from short-term ozone exposure.

A major question to be answered concerns the role of the neutrophil and other inflammatory cells in the second phase of ozone-associated epithelial injury in the conducting airways and the central acinus. The role of the neutrophil as a contributor to oxygen-induced lung injury is well documented (7), as is the experimental lung injury resulting from intrabronchial instillation of stimulated neutrophils that generate oxidants and release proteolytic enzymes into the surrounding tissue (8). No definitive evidence is available, however, on the role of the neutrophil in the ozone-induced conducting airway or centriacinar lesion. There does not appear to be any specific information on the role of neutrophils in mediating or potentiating the centriacinar injury associated with other forms of lung damage caused by inhaled toxicants (9). Both neutrophil numbers and prostaglandin (PG) products PGE_2, $PGF_{2\alpha}$, and thromboxane B_2 (TXB_2) are increased in lavage fluid of human subjects after ozone exposure (10). Neutrophils are a major source of arachidonic acid metabolites, and there is ample evidence that these metabolites may be important mediators of early inflammatory events such as those associated with exposure to ozone.

The purpose of the study was to examine the relationship between granulocyte emigration and epithelial injury in specific airway generations of the tracheobronchial tree after short-term ozone exposure in the rhesus monkey. We used an 8-h ozone exposure in monkeys followed by varying post-exposure times in filtered air to examine neutrophil emigration and accumulation in BALF and airway tissue. Morphometry of trachea and microdissected bronchi and central acini was used to define the extent of epithelial injury and repair over time after ozone exposure.

Materials and Methods

Animals

Rhesus monkeys were used in this study. All monkeys were born at the California Primate Research Center and their parentage, birth date, records of growth, and medical records were known and considered in their selection. All monkeys were male, ranging in age from 2 to 8.5 yr and weighing from 2.1 to 6.3 kg, and were given a comprehensive physical examination including a chest radiograph and complete blood count before exposure. Monkeys were transferred to exposure chambers for a 1-wk acclimatization, during which they breathed filtered air. Monkeys remained in the exposure chambers except while the chambers were cleaned each morning and during health checks. Monkeys were fed monkey chow containing 25% protein (Purina Hi-Pro) morning and evening, at which times routine health observations were also made.

Ozone Exposure and Monitoring

Monkeys were exposed individually in exposure chambers of 4.2-m^3 capacity that were ventilated at a rate of 30 changes per hour with C-B-R (chemical, biologic, and radiologic) filtered air at 24 $\pm$ 2° C and 40 to 50% relative humidity (11). Ozone concentrations were measured using an ultraviolet ozone monitor (model 1003-AH; Dasibi Environmental Corporation) and reported with respect to the UV photometric standard. Additional details of exposure and monitoring have been presented previously (4).

Experimental Protocol

Five control monkeys were exposed for 168 h to filtered air only. Fifteen monkeys were exposed for 8 h to 0.96 ppm ozone and subsequently exposed to filtered air for 1, 12, 24, 72, and 168 h of filtered air in groups of three, respectively. Monkeys with post-exposure times of 12, 24, 72, and 168 h were injected with 4×10^7 indium-labeled neutrophils suspended in 4 ml of plasma 4 h before necropsy. One hour before necropsy, filtered-air, 1- and 12-h monkeys were injected with ^3H at 1 mCi/kg. Pilot studies showed that maximal epithelial labeling occurred by 12 h after an 8-h ozone exposure in monkeys.

Neutrophil Isolation and Labeling

A total of 32 ml of blood was drawn into 8 ml of 3% sodium citrate from the cephalic veins of rhesus monkeys that had not received any drug treatment for the past 24 h before blood collection. Neutrophils were isolated from peripheral blood using discontinuous plasma-Percoll gradients layered 51 over 43% (12). Erythrocytes were removed by hypotonic lysis subsequent to gradient purification of the neutrophils. Isolated neutrophils were > 97% pure. They had > 98% viability by trypan blue exclusion and < 10% spontaneous shape change. These cells responded to the fifth component of compliment (C5) with myeloperoxidase secretion and to

phorbol myristate acetate (PMA) with oxygen radical (O_2^-) production as measured by superoxide dismutase-inhibitable cytochrome C reduction. All reagents used in the isolation of neutrophils were lipopolysaccharide (LPS) free, that is, they contained < 0.1 ng/ml of LPS using the limulus amebocyte lysate assay kit from Associates of Cape Cod (Woods Hole, MA). Isolated neutrophils were labeled with ^{111}In-chloride in an equal volume of tropolonate (5×10^{-2} M) in the presence of platelet-poor plasma. Neutrophils were washed twice and resuspended in platelet-poor plasma for reinfusion into monkeys. Blood samples were taken within 5 min and after 4 h of injection to measure circulating levels of neutrophils.

Necropsy and BAL

Monkeys were anesthetized with ketamine (30 to 35 mg/kg), administered subcutaneously, and were killed using sodium pentobarbital overdose in accordance with the Animal Care Guidelines at the California Primate Research Center. Left upper lobes were lavaged with 20 ml of sterile phosphate-buffered saline in approximately 5-ml aliquots with a recovery of 86 ± 6% of the volume infused for all monkeys in the study. The total nucleated cell count was estimated using a Coulter counter (Coulter Electronics, Hialeah, FL), and a differential count on a minimum of 200 cells was completed using a cytospin and Diff-Quik stain (American Scientific Products, McGraw Park, IL). Values were expressed as total neutrophils recovered from lavage of the lobe. The cell-free supernatant protein concentration was determined after Lowry and co-workers (13) and expressed as total protein recovered from lobar lavage. A gamma well counter was used to measure ^{111}In-labeled neutrophils in BALF cell pellets, the left upper lung lobe, liver, spleen, and tracheobronchial lymph nodes.

Morphometry

The right upper lobe of each monkey was cannulated and instilled with a glutaraldehyde-paraformaldehyde fixative in 0.2 μm cacodylate buffer (330 mOsm) at 30 cm of water pressure. The lower third of the tracheas were fixed in the same fixative. After a minimum of 12 h of fixation, airways were microdissected to obtain the fourth- and ninth-generation bronchi and fifteenth-generation respiratory bronchioles from the right upper lobe of each monkey (14). Samples were also taken from each trachea. All samples were bisected along their longitudinal axis, postfixed in 1% osmium tetroxide, dehydrated in a series of ethanol baths and embedded in Araldite. One-micron sections were cut from each airway so that the epithelium was cut perpendicular to the basal lamina and then stained with toluidine blue. Two blocks were selected by stratified sampling from each airway, making sure that the epithelium was cut perpendicular to its basal lamina. Sections from these small blocks (1- to 2-mm face) were placed on grids and stained with uranyl acetate and lead citrate before viewing on a Zeiss EM-10A transmission electron microscope. Ten micrographs were taken, five from epithelium and five from interstitium (one microscopic field beneath the epithelium for trachea and bronchi, whereas the total interstitium was taken for respiratory bronchioles) using area-weighted periodic sampling at 3,800× magnification (15). A cycloid grid was placed so that its vertical axis was perpendicular to the epithelial basal lamina, and point "hits" were counted on all epithelial and interstitial cells and extracellular components while intersections of the epithelial basal lamina were recorded on the same fields. Epithelial cells in the trachea and bronchi included ciliated, mucous, small mucous granule, basal, and necrotic/degenerating cells (16). Epithelial cells in respiratory bronchioles included ciliated, nonciliated bronchiolar, type I epithelial, type II epithelial, and necrotic/degenerating cells (4). Point "hits" on inflammatory cells (neutrophils, eosinophils, and mononuclear phagocytes/alveolar macrophages) in direct contact with epithelial cells either in the epithelial intercellular space or apical surface were counted. Interstitial cells included fibroblasts, smooth muscle cells, capillary, lymphatic small vessel endothelial cells (including their lumina), and nerve cell bodies and processes. Extracellular components of the interstitium included collagenous fibers, elastic fibers, and amorphous ground substance. Inflammatory cells in the interstitial compartment included neutrophils, eosinophils, lymphocytes, mast cells, and mononuclear phagocytes.

The volume density of individual epithelial cells and inflammatory cells ($V_{V_{cell,\ epi}}$) in the epithelial compartment to the total epithelial compartment (epithelium and inflammatory cells) was calculated by point counting as follows (17):

$$V_{V_{cell,\ epi}} = \frac{P_{cell}}{P_{epi}}$$

where P_{cell} are the points that "hit" individual cells and P_{epi} are all of the point "hits" in the epithelial compartment. The volume density of cells and extracellular components of the interstitium were calculated in a similar manner except that small vessels, capillaries, lymphatics, and nerves were not included because of their wide variability in airway walls. The surface area of the epithelial basal lamina to either the epithelium or interstitial volume ($S_{V_{bl,\ epi}}$ or $S_{V_{bl,\ int}}$) was calculated by point and intersection counting as follows (18):

$$S_{V_{bl,\ epi}} = \frac{2I_{bl}}{L_{epi}}$$

where I_{bl} are intersections of the test line of the cycloid grid with the epithelial basal lamina and L_{epi} is the test line length over the epithelial compartment. To compare epithelial cells and inflammatory cells between airways and over time, we normalized the volume of the epithelial or interstitial cells by the epithelial basal laminar surface area ($V_{S_{cell,\ bl}}$) as follows:

$$V_{S_{cell,\ bl}} = \frac{V_{v_{cell,\ epi}}}{S_{V_{bl,\ epi}}}$$

where the reference volumes are the same and divide to 1. This method of normalization was also used to evaluate the interstitial compartment of the respiratory bronchiole since we sampled the entire compartment. Four stratified samples (blocks) were also taken from the right upper lobe for histopathologic evaluation.

Autoradiography

Epon-Araldite sections, 1.5 μm thick, from each of the airway samples, were mounted on glass slides and coated with a 1:1 solution of Ilford L-4 emulsion and distilled water. They were dried and stored in light-tight boxes at 0 to 4° C for 4 wk. Emulsions were then developed in 13.5% Microdol X

for 10 min, fixed in 15% sodium thiosulfate for 10 min, and washed in water for 20 min. Sections were stained with toluidine blue, and a coverslip was mounted. A minimum of 1,000 nucleated epithelial cells (range, 1,000 to 4,000) was counted for each airway level (trachea, bronchi, and respiratory bronchiole) for each monkey at 1,000×. In order for a cell to be classified as labeled, a minimum of five silver grains superimposed on the nucleus was required.

Detection of Prostaglandins

From BALF supernatant, derivatized analytes and internal standards were detected by simultaneous monitoring of ions at six different masses characteristic for each of the derivatized prostanoids using capillary gas chromatography-negative ion chemical ionization mass spectrometry as described (19). Briefly, 1 ml of BALF supernatant containing 0.8 to 2.0 ng of deuterated analogs of PGE_2, $PGF_{2\alpha}$, and 6-keto-$PGF_{1\alpha}$ to 4-ml of high performance liquid chromatography (HPLC)-grade absolute methanol was placed in a silanized 25-ml centrifuge tube, chilled for 15 min on ice, and centrifuged at 2,500 rpm for 10 min. The supernatant was decanted into a second 25-ml silanized centrifuge tube and added q.s. with HPLC-grade water to 20 ml total volume. The tube was warmed to room temperature. A SEP-PAK C_{18} cartridge was charged with 10 ml of HPLC-grade methanol followed by a rinse with 10 ml of HPLC-grade water. Next, the SEP-PAK was loaded with 20 ml of sample and the effluent was discarded. The SEP-PAK was then flushed with 10 ml of 20% HPLC-grade methanol. The SEP-PAK C_{18} was eluted with 4 ml of 80% methanol, which was collected in a silanized vial with a teflon insert cap. After drying under a nitrogen stream, the extract with internal standards was sequentially derivatized for vapor-phase analysis and detection of characteristic negatively charged fragment ions of 9α,11β-PGF_2, $PGF_{2\alpha}$, PGD_2, PGE_2, TXB_2, and 6-keto-$PGF_{1\alpha}$ as described (19).

Mucus Release in BALF Supernatant

A panel of monoclonal antibodies to rhesus monkey airway secretions (20) was used in an enzyme-linked immunosorbent assay (ELISA) system to measure nanogram levels of mucus released from airway secretory cells. Our ELISA method is a double-sandwich method. Briefly, 200 μl of each monoclonal antibody (ascites fluid that has been purified in a DEAE sephacell column; final concentration, 1 μg/ml) was coated onto the center 60 wells of a 96-well Immulon plate and incubated for 3 h at 37° C. The plates were washed with phosphate-buffered saline containing 0.05% Tween® 20 (TPBS). The plates were stored at 4° C until used. When ready, the test sample or standard mucin were applied to each well (200 μl/well) and incubated for 4 h at 37° C or overnight at 4° C. The plates were washed with TPBS, then 200 μl of each enzyme-antibody conjugate was applied to each well for 4 h or overnight as above. Each purified monoclonal antibody was conjugated with alkaline phosphatase using glutaraldehyde. After the enzyme-antibody conjugate was washed from the wells, 200 μl of *p*-nitrophenylphosphate substrate was added. The plates were incubated at room temperature and then read at 405 nm on a Dynatech M-R 600 microplate reader. Readings were taken at 15, 30, 60, and 90 min. The reaction was linear over this length of time. A standard curve was then constructed, and values for the amount of secretory product contained in lavage were determined.

Statistical Analysis of Data

Prostaglandin and mucus data on BALF supernatant, counts per minute of ^{111}In in lung tissue, and BALF-recovered cells were expressed on the basis of total lavage fluid volume recovered per left upper lung lobe. The values were reported as the mean ± 1 SEM. BALF, tissue ^{111}In, and morphometric data were analyzed by one-way ANOVA and the Duncan's multiple comparison test (21). The prostaglandin data were not normally distributed and were analyzed by nonparametric statistics (Kruskal Wallis and Mann Whitney U tests) (21). A value of $P \leq 0.05$ was considered significant.

Results

Filtered Air and One Hour after Exposure

Light and transmission electron microscopy showed normal epithelium and interstitium for the trachea, bronchi, and respiratory bronchioles for all monkeys exposed to filtered air (Figure 1). In airways of monkeys exposed to 8 h of 0.96 ppm ozone followed by 1 h in filtered air, epithelial necrosis was evident in the trachea, bronchi, and respiratory bronchioles (Figure 2). Morphometry only showed a significant increase in necrotic cells in trachea and respiratory bronchioles (Figures 3 and 4). Ciliated cells were markedly reduced by 1 h after exposure in the trachea and bronchi, but only in the bronchi were basal cells decreased in volume as compared with filtered-air controls. Cilia were lost from ciliated cells, leaving the appearance of short or no cilia with a prominent row of basal bodies in the apical cytoplasm. Occasional granulocytes were observed within the surface epithelium of the trachea and bronchi, but granulocytes were more numerous in respiratory bronchioles. Only alveolar macrophages adjacent to respiratory bronchiolar epithelium showed a marked increase in volume at the 1-h post-exposure time as compared with filtered-air controls (Figures 5 through 7). Goblet cells of the trachea and bronchi contained fewer secretory granules; however, only in the trachea were they markedly decreased in volume (Figure 3). It is noteworthy that mucins detected by an ELISA method in BALF supernatant were significantly increased as compared with the filtered-air controls in the 1-h post-exposure monkeys (Table 1). Respiratory bronchioles also showed extensive cellular debris in their airways and numerous vacuoles in low cuboidal epithelium. The epithelial cell nuclei had a euchromatin appearance with prominent nucleoli. The interstitium was moderately swollen and contained numerous granulocytes. These changes in the epithelium of conducting and distal airways were associated with marked increases in lavagable prostaglandins, with $PGF_{2\alpha}$, PGD_2, and PGE_2 significantly increased as compared with filtered-air controls (Table 2). The total number of cells and neutrophils recovered from BALF was significantly increased at the 1-h post-exposure times compared with filtered-air monkeys (Table 1).

Twelve Hours after Exposure

In the trachea, there was a marked increase in the intercellular space. This was associated with aggregations of neutro-

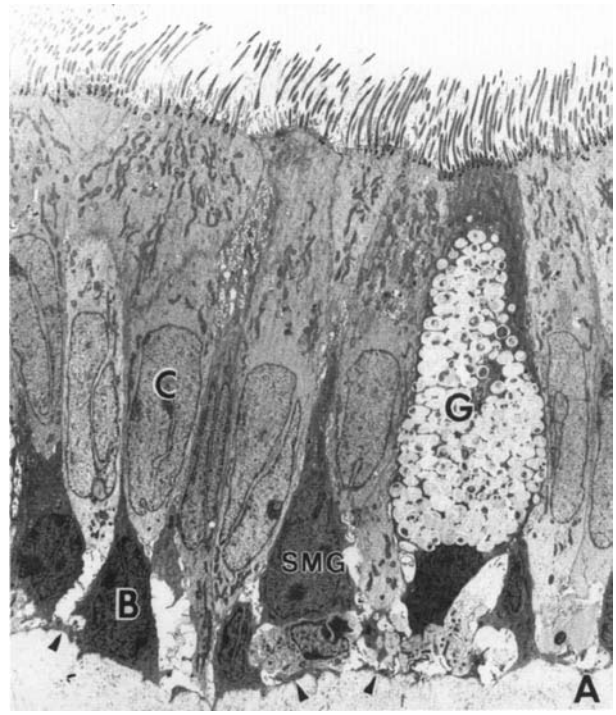

Figure 1. Normal appearance of epithelium and interstitium of airways from a monkey exposed to filtered air for 7 days. *Panel A:* Trachea. Note the columnar epithelium composed of ciliated (C), goblet (G), small mucous granule (SMG), and basal (B) cells. Note the basal bodies along the apical surface of the ciliated cells and cilia in the tracheal lumen. Arrowheads mark the epithelial basal lamina. Magnification: ×1,776. *Panel B:* Segmental bronchus. Note that all of the cell types found in the trachea are present; interstitial cells (I) are found beneath the basal lamina. Magnification: ×2,412. *Panel C:* A first-generation respiratory bronchiole shows a low cuboidal epithelium toward the respiratory bronchiole lumen (RB). A type I (I) epithelial cell lines an alveolar outpocket. Note the large groups of smooth muscle cells (SM), occasional fibroblast (F), and collagenous fibers (CT) in the interstitium. Magnification: ×1,575.

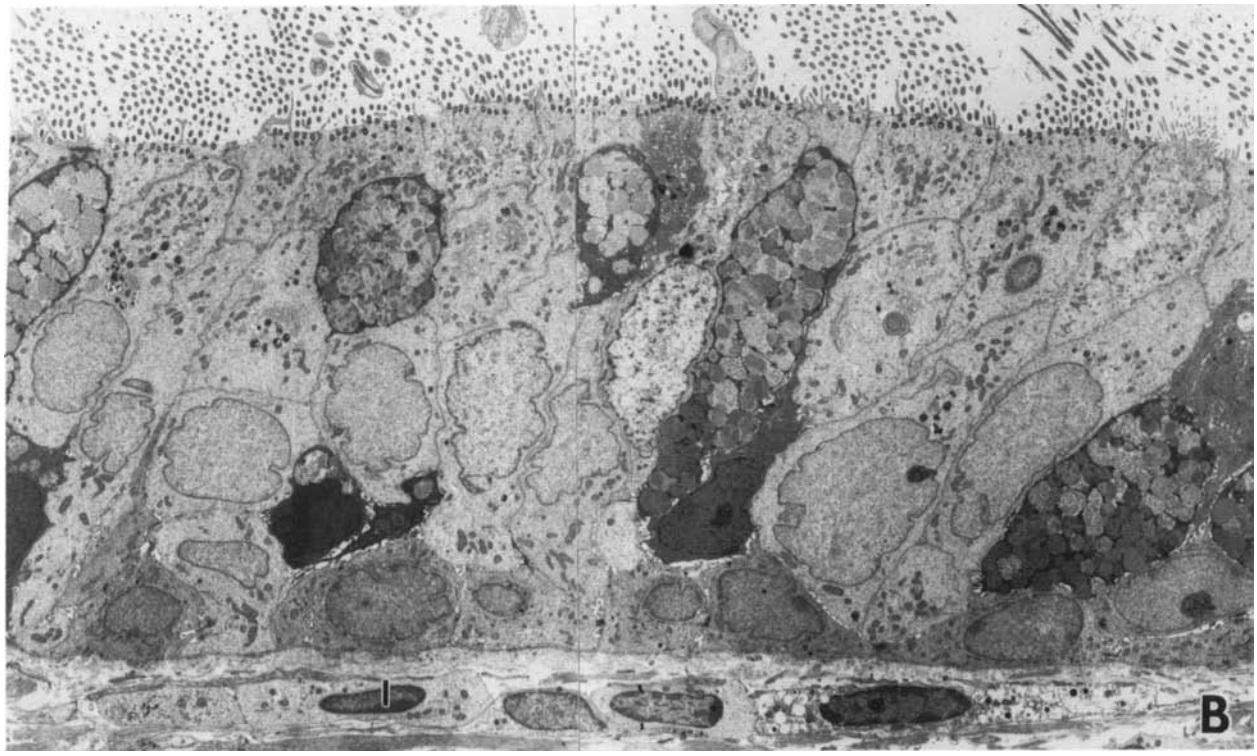

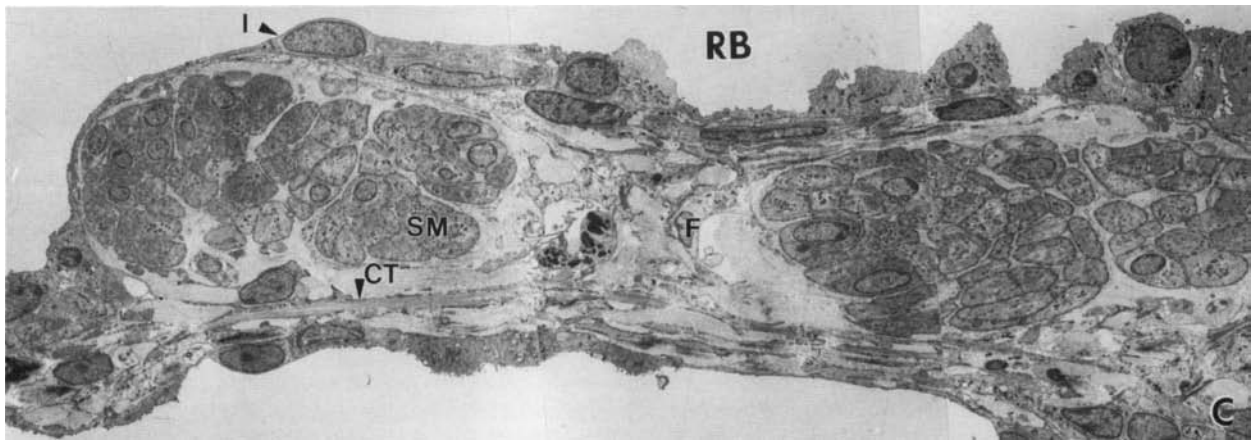

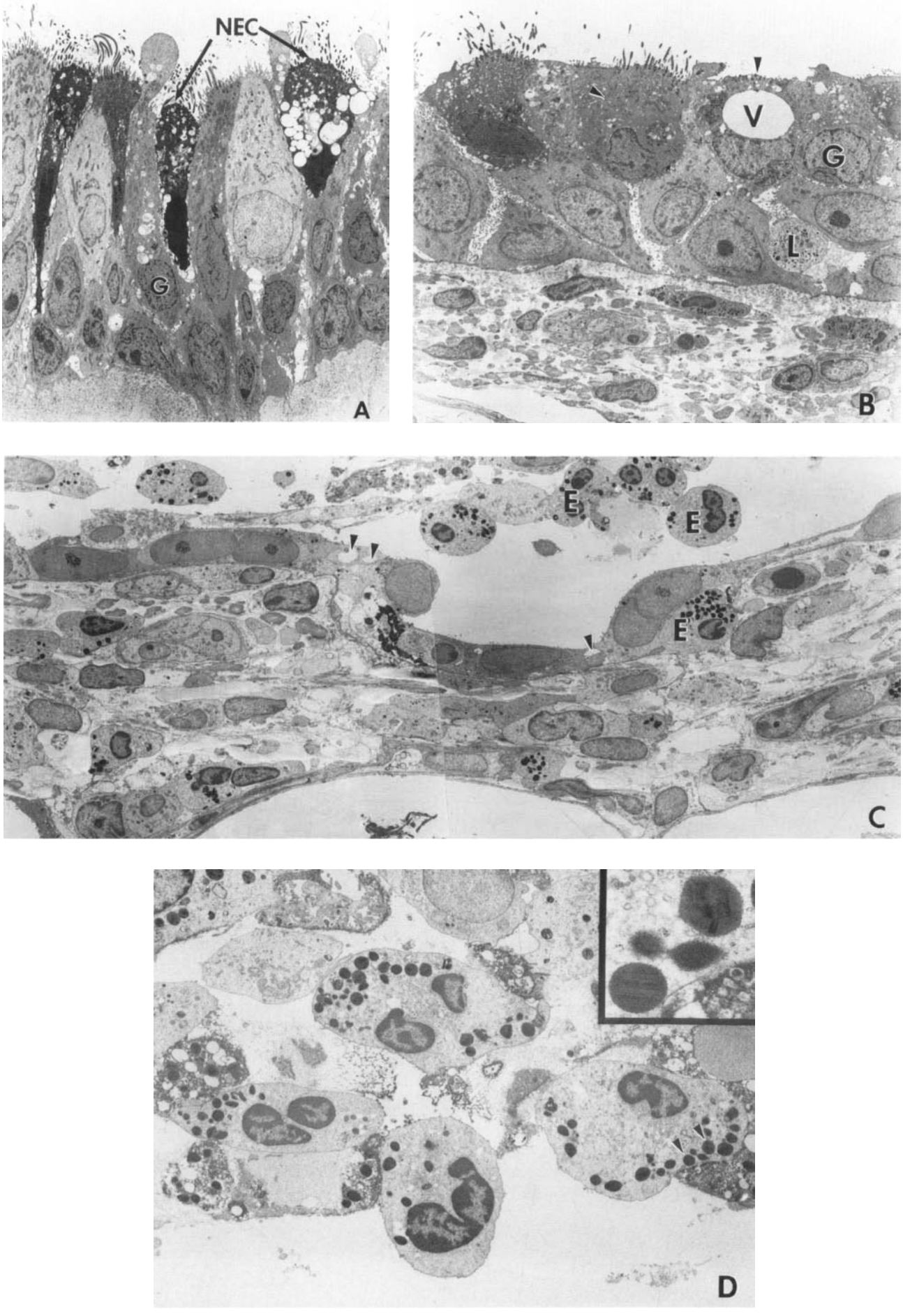
NEC
G
A
V
G
L
B
E
E
E
C
D

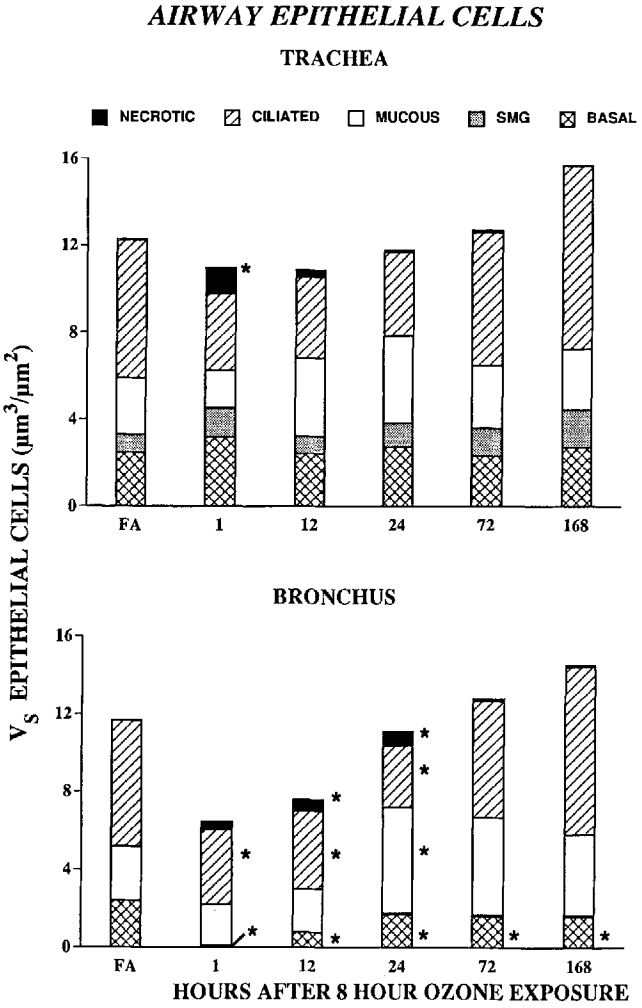

Figure 3. The volume of airway epithelial cells in trachea and bronchi per surface area of epithelial basal lamina (V_s) in monkeys exposed to only filtered air (FA) or 0.96 ppm ozone for 8 h followed by 1, 12, 24, 72, or 168 h in filtered air. Bars represent mean values. SMG = small mucous granule cell. * Significantly different ($P \leq 0.05$) than filtered-air monkeys.

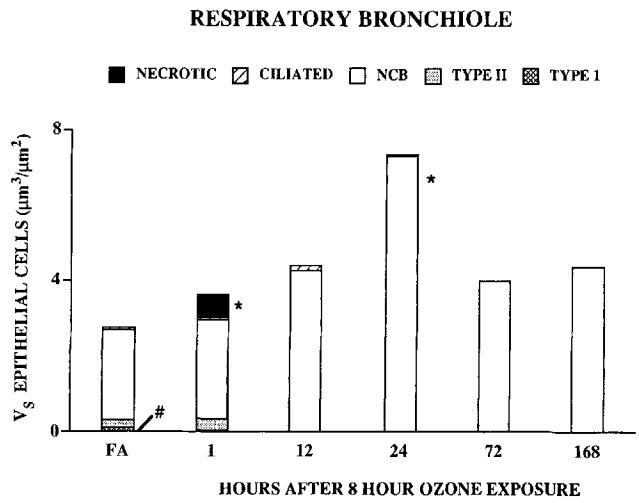

Figure 4. The volume of epithelial cells per surface area of epithelial basal lamina (V_s) in respiratory bronchioles in monkeys exposed to only filtered air (FA) or 0.96 ppm ozone for 8 h followed by 1, 12, 24, 72, or 168 h in filtered air. Bars represent mean values. NCB = nonciliated bronchiolar cell. * Significantly greater ($P \leq 0.05$) than filtered-air monkeys. # Significantly greater ($P \leq 0.05$) V_s of type I epithelial cells than 12, 24, 72, and 168 h.

phils and loss of ciliated cells (Figures 3, 5, and 8A). In these locations, neutrophils were also accumulated directly beneath the basal lamina. Neutrophil volume per epithelial basal laminar surface area was increased in both epithelial and interstitial compartments (Figure 5). Sloughed and necrotic epithelial cells were also observed, although they were less than in the 1-h post-exposure animals (Figure 3).

Many dome-shaped undifferentiated cells were observed in the epithelium. Their surface was covered with short microvilli, and their nuclei were euchromatic with a prominent nucleolus (Figure 8A). In general, bronchi showed a more severe lesion at this time than the trachea. Although intercellular spaces were not enlarged (Figure 8B), there were significantly more necrotic cells and fewer ciliated and basal cells in the bronchial epithelium (Figure 3). Eosinophils were markedly increased in both epithelial and interstitial compartments, whereas neutrophils were only increased in the bronchial epithelium at this time compared with filtered-air controls (Figure 6). In all monkeys at this time, respiratory bronchioles were similar in appearance to the 1-h post-exposure group, but only type I epithelial cells were significantly decreased (Figure 4). Ciliogenesis was evident by the appearance of numerous basal bodies in the cytoplasm of the cuboidal epithelium (Figure 8C). Although all inflammatory cell types were observed in both compartments, only eosinophils were significantly increased as compared with filtered-air controls (Figure 7). At all airway levels except the respiratory bronchioles, the labeling index for epithelial cells was markedly increased, significantly for bronchi, as compared with filtered-air controls (Figure 9).

Figure 2. Airways from monkeys exposed to 8 h of 0.96 ppm ozone followed by 1 h of filtered air. *Panel A:* Trachea. Note the necrotic epithelial cells (NEC) and loss of apical cilia on ciliated cells (*arrows*). Note the reduced number of mucous granules in goblet cells (G). Magnification: ×1,620. *Panel B:* Bronchus. Note the loss of apical cilia on ciliated cells (*arrowheads*) and reduced number of mucous granules in goblet cells (G). Note large vacuoles (V) in ciliated cell and a leukocyte (L) in the epithelium. Magnification: ×1,786. *Panel C:* Respiratory bronchiole. Cellular debris, eosinophils (E), neutrophils, and alveolar macrophages mark the lumen of a first-generation respiratory bronchiole. Note the numerous vacuoles (*arrowheads*) in the low cuboidal epithelium lining the respiratory bronchiole lumen. The epithelial cell nuclei have a euchromatin appearance with prominent nucleoli. Note the granulocytes in the interstitium. Magnification: ×1,786. *Panel D:* Respiratory bronchiole. Eosinophils in the interstitium are characterized by their crystallin core (*arrowheads and inset*). Magnification: ×4066; inset: ×19,760.

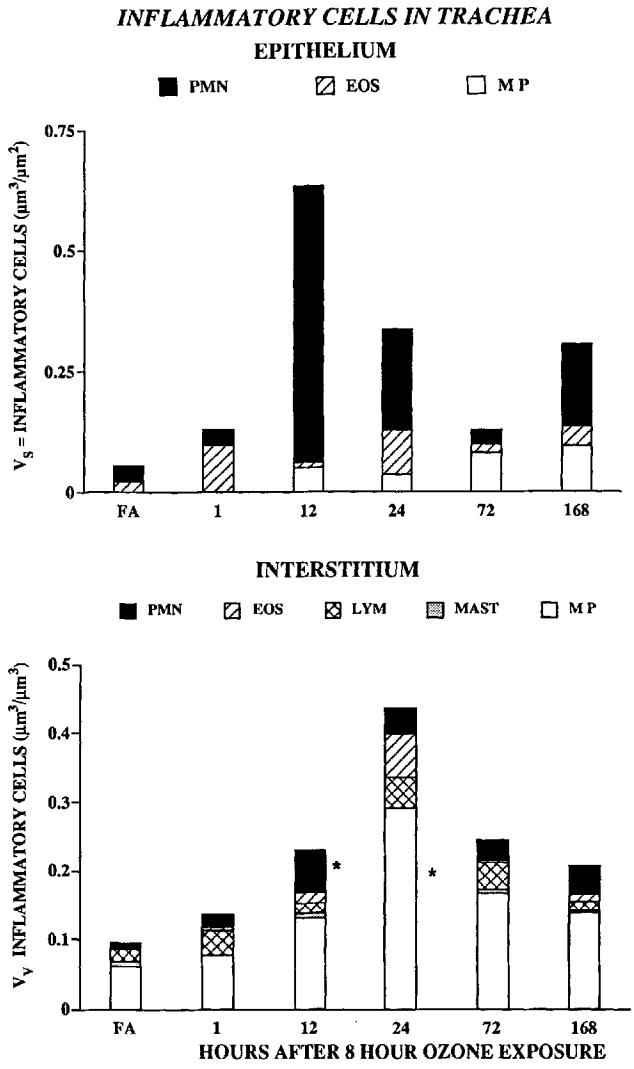

Figure 5. The volume of inflammatory cells per surface area of epithelial basal lamina (V_s) in the epithelium and per volume (V_v) of interstitium in the trachea of monkeys exposed to only filtered air (FA) or 0.96 ppm ozone for 8 h followed by 1, 12, 24, 72, or 168 h in filtered air. Bars represent mean values. PMN = neutrophil, EOS = eosinophil, MP = mononuclear phagocyte, and LYM = lymphocyte. * Significantly greater ($P \leq 0.05$) than filtered-air monkeys.

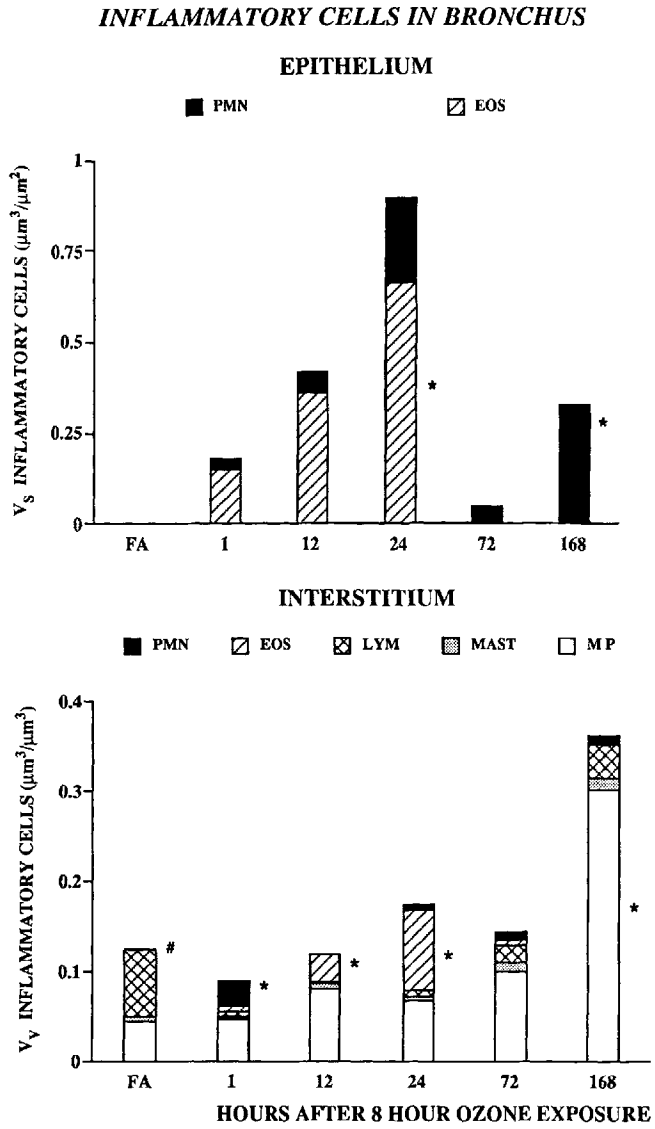

Figure 6. The volume of inflammatory cells per surface area of epithelial basal lamina (V_s) in the epithelium and per volume (V_v) of interstitium in bronchi of monkeys exposed to only filtered air (FA) or 0.96 ppm ozone for 8 h followed by 1, 12, 24, 72, or 168 h in filtered air. Bars represent mean values. PMN = neutrophil, EOS = eosinophil, LYM = lymphocyte, and MP = mononuclear phagocyte. * Significantly greater ($P \leq 0.05$) than filtered-air monkeys. # Significantly greater ($P \leq 0.05$) than all other times.

Neutrophil migration was at its peak at 12 h after exposure. Neutrophils were observed within the epithelium and in the interstitium directly beneath the epithelium of all airway levels at this time (Figures 5 through 7). The percentage of ^{111}In-labeled neutrophils was significantly greater in BALF-recovered cells and in lung tissue at 12 h after exposure as compared with filtered-air controls (Figure 10). Neutrophils used for ^{111}In-labeling and reinfusion showed circulatory kinetics of 48 ± 2% of the cells injected intravenously after 5 min and 16 ± 4% after 4 h (Table 3). The remainder of ^{111}In-labeled neutrophils was found in the liver and spleen at necropsy. No significant difference was observed in ^{111}In-labeled neutrophils in tracheobronchial lymph nodes at 12 h after exposure (Table 3). The total number of cells, as well as neutrophils in BALF, was significantly greater in exposed animals than in filtered-air monkeys (Table 1).

Twenty-four Hours after Exposure

Repair of tracheal epithelium was evident by 24 h after the end of exposure (Figure 11A). Ciliated pseudostratified columnar epithelium with ciliated, goblet, and basal cells comprised the tracheal epithelium. Necrotic epithelial cells were infrequently observed, and evidence of ciliogenesis was indicated by the number of cells with disorganized basal bodies in their apical cytoplasm. Neutrophils and eosinophils were still commonly observed in the epithelium, but

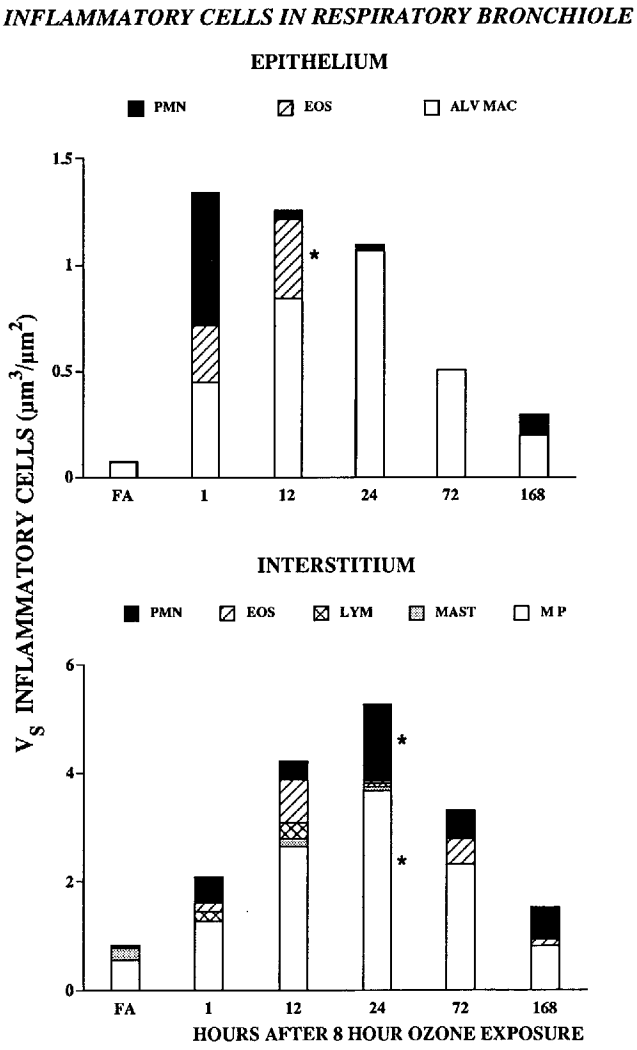

Figure 7. The volume of inflammatory cells per surface area of epithelial basal lamina (V_s) in epithelium and interstitium of respiratory bronchioles of monkeys exposed to only filtered air (FA) or 0.96 ppm ozone for 8 h followed by 1, 12, 24, 72, or 168 h in filtered air. Bars represent mean values. PMN = neutrophil, EOS = eosinophil, ALV MAC = alveolar macrophage, LYM = lymphocyte, and MP = mononuclear phagocyte. * Significantly greater ($P \leq 0.05$) than filtered-air monkeys.

only in the tracheal interstitium were mononuclear phagocytes significantly increased (Figure 5). In contrast to the trachea, bronchial inflammation and epithelial necrosis were greater than at 12 h after exposure. Bronchial epithelium had a disorganized appearance with some luminal necrotic cells, undifferentiated cells in the more basal regions, and numerous neutrophils and eosinophils (Figure 11B). There was a notable increase in necrotic cells and a significant decrease in ciliated and basal cells in the bronchial epithelium (Figure 3). In both epithelial and interstitial compartments, there were significant increases in eosinophils (Figure 6). Bronchiolar regions showed areas of epithelial loss and neutrophils and eosinophils in the adjacent airspace. Hypertrophy of nonciliated bronchiolar cells was observed and correlated with a significantly greater cumulative cell volume per epithelial basal laminar surface area as compared with controls (Figure 4). Although some areas of the interstitium were similar to those of controls (Figure 11C and Table 5), there was a significant increase in neutrophils and mononuclear phagocytes (Figure 7). Epithelial loss and occasional large alveolar macrophages with numerous inclusions were observed in proximal alveolar ducts (Figure 11D). The total number of cells, including neutrophils, in BALF was significantly greater than in filtered-air monkeys but was similar to that in 12-h post-exposure animals (Table 1). In contrast, ^{111}In-labeled neutrophils in lung tissue and BALF were not significantly greater than in filtered-air monkeys (Figure 10).

Three Days after Exposure

The tracheal epithelium did not differ from controls by 3 days after the end of exposure (Figure 3), and repair of bronchial and respiratory bronchiolar epithelium was apparent (Figures 3 and 4). Necrotic ciliated cells were still encountered in the bronchial epithelium at 3 days after exposure (Figure 3). Numerous cells with disorganized basal bodies in their apical cytoplasm and numerous undifferentiated cells were present in bronchi (Figure 12A). Neutrophils and eosinophils were decreased in numbers compared with previous times but were still present in the interstitium (Figures 6 and 7). Respiratory bronchioles contained osmiophilic collagenous fibers in the interstitium (Figure 12B). The total number of cells, including lymphocytes, in BALF was

TABLE 1

*Leukocytes, total protein, and mucin recovered by bronchoalveolar lavage after ozone exposure**

Exposure Groups	Monkeys (*n*)	Total Cells ($\times 10^{-6}$)	Neutrophils ($\times 10^{-6}$)	Macrophages ($\times 10^{-6}$)	Lymphocytes ($\times 10^{-6}$)	Protein (*mg*)	Mucin (μg)
FA	5	3.12 ± 0.653	0.10 ± 0.040	2.92 ± 0.644	0.05 ± 0.045	1.385 ± 0.1806	0.416 ± 0.1224
8 h O_3 + 1 h FA	3	6.21 ± 1.057†	2.71 ± 0.219†	3.50 ± 1.034	0.00 ± 0.00	3.565 ± 0.9946	1.984 ± 0.2930†
8 h O_3 + 12 h FA	3	6.17 ± 0.185†	1.93 ± 0.208†	4.24 ± 0.179	0.00 ± 0.00	3.516 ± 0.9492	0.482 ± 0.1401
8 h O_3 + 24 h FA	3	6.71 ± 0.185†	2.45 ± 0.866†	4.20 ± 0.728	0.06 ± 0.029	10.865 ± 4.0723†	0.607 ± 0.1978
8 h O_3 + 72 h FA	3	5.99 ± 1.738†	0.61 ± 0.185	5.03 ± 1.478	0.35 ± 0.087†	3.978 ± 2.1099	0.883 ± 0.3314
8 h O_3 + 168 h FA	3	1.97 ± 0.283	0.29 ± 0.017	1.63 ± 0.318	0.05 ± 0.023	1.309 ± 0.2154	N

Definition of abbreviations: FA = filtered air; O_3 = ozone; N = not measured.
* All values are mean ± 1 SEM. Macrophages include monocytes observed in lavage (< 3%).
† Significantly greater than ($P \leq 0.05$) those filtered-air controls.

TABLE 2
*Prostaglandins recovered from bronchoalveolar lavage fluid after ozone exposure**

Exposure Groups	Monkeys (*n*)	9α,11β-PGF_2	$PGF_{2\alpha}$	PGD_2	PGE_2	TXB_2	6k $PGF_{1\alpha}$
FA	5	24.60 ± 15.071	200.40 ± 126.083	37.20 ± 23.094	87.30 ± 53.692	13.50 ± 13.501	39.30 ± 32.012
8 h O_3 + 1 h FA	3	634.00 ± 507.75	10,144.00 ± 9,299.35†	368.67 ± 118.41†	888.67 ± 48.26†	2,323.33 ± 2,243.8	1,020.00 ± 924.04
8 h O_3 + 12 h FA	3	54.00 ± 39.104	366.17 ± 71.955	149.33 ± 72.221	446.00 ± 170.570	26.67 ± 26.668	170.33 ± 85.165
8 h O_3 + 24 h FA	3	224.00 ± 200.479	541.33 ± 501.868	1,426.67 ± 1,426.63	306.67 ± 306.665	48.00 ± 48.001	552.00 ± 551.999
8 h O_3 + 72 h FA	3	119.33 ± 60.668	982.67 ± 474.668	86.00 ± 48.538	483.33 ± 204.457	113.33 ± 56.961	153.33 ± 153.333
8 h O_3 + 168 h FA	3	22.50 ± 22.50	265.00 ± 264.998	7.50 ± 7.500	57.50 ± 57.500	0.00 ± 0.00	0.00 ± 0.000

Definition of abbreviations: FA = filtered air; O_3 = ozone; 9α,11β-PGF_2 = 15(S),9α,11β-trihydroxyprosta-5Z, 13 E-dien-1-oic acid; $PGF_{2\alpha}$ = prostaglandin $F_{2\alpha}$; PGD_2 = prostaglandin D_2; PGE_2 = prostaglandin E_2; TXB_2 = thromboxane B_2; 6k $PGF_{1\alpha}$ = 6-keto-prostaglandin $F_{1\alpha}$.

* All values are mean ± 1 SEM in nanograms for the left cranial lung lobe.

† Significantly greater ($P \ll 0.05$) than filtered-air control.

significantly greater than in filtered-air monkeys (Table 1). Most of the increase in total BALF cells was from increased alveolar macrophages and not lymphocytes.

Seven Days after Exposure

By 7 days after the end of exposure, the appearance of the epithelium, the trachea, bronchi, respiratory bronchioles, and proximal alveolar ducts did not differ from controls. Bronchial epithelium showed a marked increase in the volume of ciliated and mucous cells, whereas the volume of basal cells was significantly decreased per basal laminar surface area. Some necrotic epithelial cells were observed (Figure 3). Marked increases in eosinophils in tracheal interstitium and neutrophils in bronchial epithelium and interstitium were observed (Figures 5 and 6). Mononuclear phagocytes were also significantly increased in bronchial interstitium as compared with those of controls (Figure 6). The interstitium appeared of normal thickness and composition except for the occasional appearance of osmiophilic collagenous fibers in respiratory bronchioles (Tables 4 and 5). The total number of cells, including alveolar macrophages, in BALF was less than in filtered-air monkeys (Table 1).

Discussion

The present study has four novel observations in the evaluation of acute ozone-induced injury to tracheobronchial epithelium: (*1*) the sequence of epithelial injury and repair differed by airway generation, occurring earlier in the trachea and respiratory bronchioles than in bronchi; (*2*) there was a strong relationship between epithelial necrosis and the emigration and retention of neutrophils at all levels of the tracheobronchial tree; (*3*) there was a strong association between maximal epithelial necrosis, BALF protein levels, and granulocytes (especially eosinophils) in bronchi, but not the trachea and bronchioles; and (*4*) there was a strong relationship between increased mucin in BALF and loss of mucous granules in goblet cells of the tracheobronchial epithelium.

The earlier time course of injury and repair in the trachea and respiratory bronchioles as compared with bronchi was an unexpected observation. To the best of our knowledge, this is the first such report comparing epithelial injury and repair between different airway levels after short-term ozone exposure. The net dose and removal (as much as 40%) of ozone is higher in more proximal conducting airways than more distal airways (22); whether this can explain why the trachea showed an earlier time of injury and repair is doubtful. Tracheal epithelial necrosis and a significant decrease in ciliated cells occurred at 1 h after the 8-h ozone exposure when granulocytes in the tracheal epithelium and interstitium were not markedly increased. This result is best explained by direct ozone-induced epithelial injury in the trachea. Although our data suggest that neutrophil accumulation in the ozone-injured trachea by 12 h after exposure is an epiphenomenon to epithelial injury, it is likely that neutrophils assist in killing ozone-injured epithelial cells. Neutrophil-mediated tissue injury is well characterized *in vivo*. *In vivo* evidence of oxidant generation and proteolytic enzyme release from stimulated neutrophils has been demonstrated in experimental lung injury induced by the administration of formulated norleu-leu-phe (FNLP) intrabronchially and PMA intravenously to rabbits (8). Oxidants

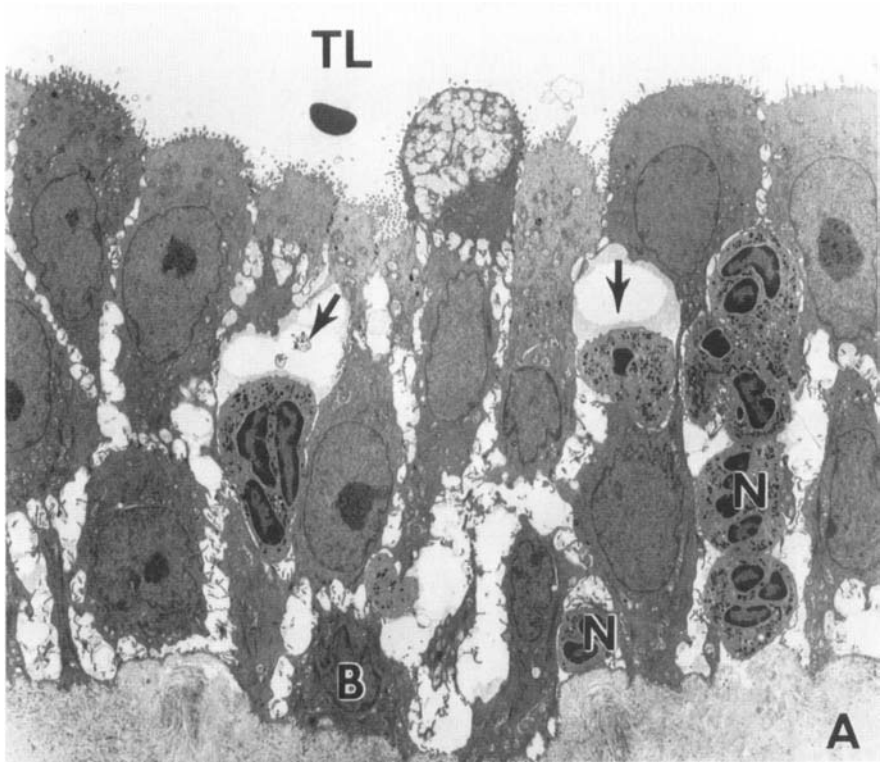

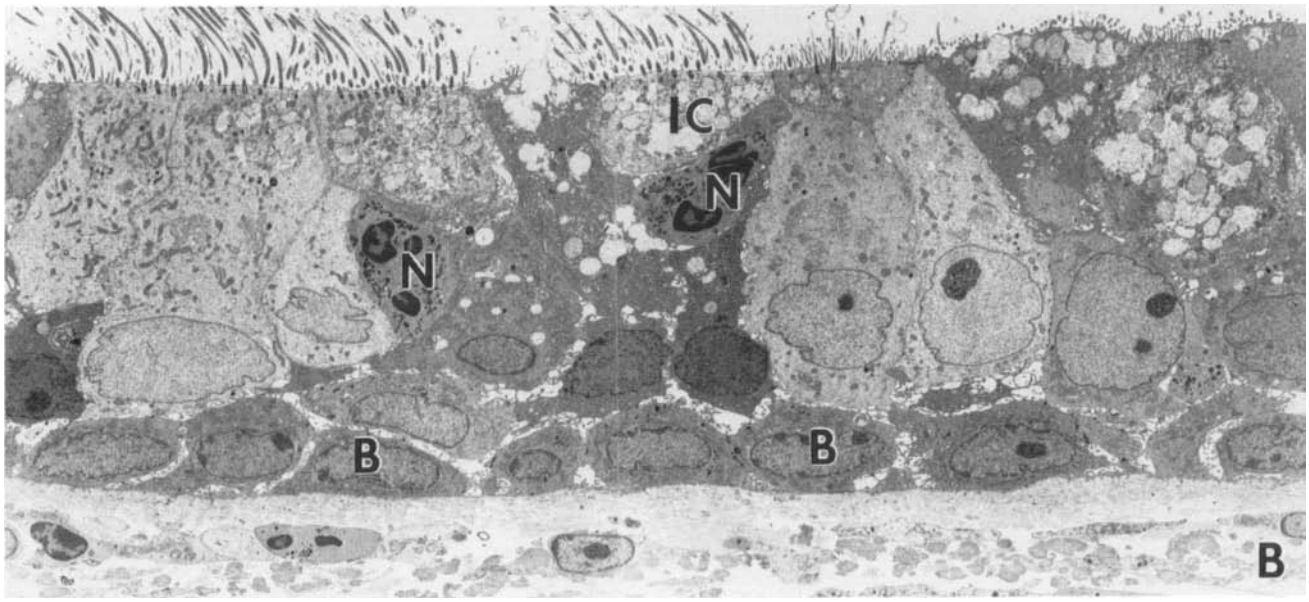

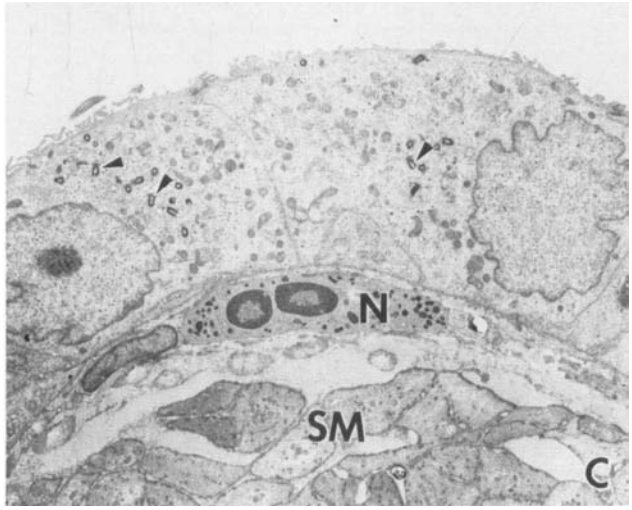

Figure 8. Airways from monkeys exposed to 8 h of 0.96 ppm ozone followed by 12 h of filtered air. *Panel A:* Trachea. Note the expanded intercellular spaces (*arrows*) and numerous neutrophils (N) between epithelial cells. The epithelium is comprised primarily of small mucous granule cells in the apical region, while basal cells (B) are still well defined. TL = tracheal lumen. Magnification: ×2,295. *Panel B:* Bronchus. Note the ciliated pseudostratified appearance of the epithelium. Basal cells (B) and some ciliated cells (C) have a normal appearance, while there are some intermediate cells (I) that have mucous-like inclusions and cilia or basal bodies in the apical cytoplasm. Two neutrophils (N) are seen intercellularly, but the intercellular space is not abnormally dilated. Magnification: ×2,210. *Panel C:* Respiratory bronchiole. Note the basal bodies (*arrowheads*) in the undifferentiated cuboidal epithelium. In the interstitium, a neutrophil (N) is beneath the basal lamina and adjacent to numerous smooth muscle cells (SM). Magnification: ×3,723.

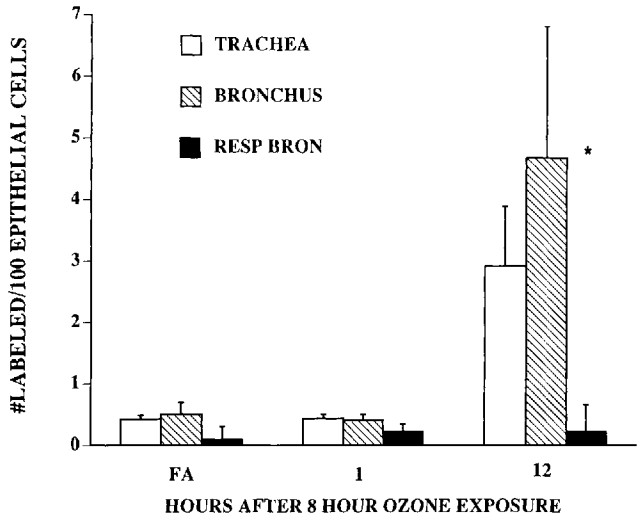

Figure 9. The labeling index (number of labeled cells per 100 epithelial cells) for trachea, bronchi, and respiratory bronchioles (RESP BRON) of monkeys exposed to only filtered air (FA) or 0.96 ppm ozone for 8 h followed by 1 or 12 h in filtered air. Bars are mean ± SEM. * Significantly greater ($P \leq 0.05$) than filtered-air monkeys.

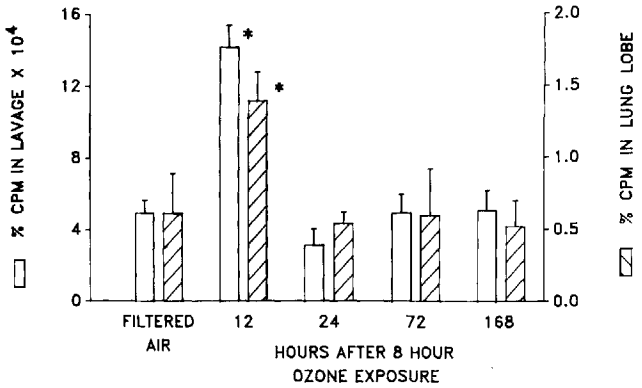

Figure 10. The percentage of ^{111}In-labeled neutrophils per total cpm infused intravenously in bronchoalveolar lavage or in the left upper lung lobe of monkeys exposed to filtered air or 0.96 ppm ozone followed by 12, 24, 72, or 168 h in filtered air. Bars are mean ± SEM. * Significantly greater ($P \leq 0.05$) than filtered-air monkeys.

and neutrophil elastase have also been demonstrated in the BALF from patients with the adult respiratory distress syndrome (ARDS) (23, 24). The repair of the tracheal epithelium by 12 h after ozone exposure was associated with the greatest neutrophil volume in the epithelium. The influence of neutrophils on epithelial repair is poorly characterized. It has been shown that neutrophil defensins (including corticostatin), which are localized in azurophilic granules and are best known for their antimicrobial properties, also stimulate DNA synthesis in cultured lung cell lines (25–27). If neutrophil defensins play a role in epithelial repair, neutrophils could be considered as beneficial in ozone-induced injury by enhancing removal of ozone-injured epithelial cells and by stimulating proliferation of the remaining epithelial stem cells.

A similar interpretation can be made for epithelial cells of respiratory bronchioles. Significant necrosis of epithelial cells of respiratory bronchioles was only observed 1 h after the 8-h ozone exposure, which is also indicative of direct ozone-induced injury. There was not a significant increase in thymidine incorporation into epithelial cells of respiratory bronchioles, but this was not unexpected because nonciliated bronchiolar cells showed no detectable labeling index in bonnet monkeys exposed continuously to ozone (0.8 ppm) for 4, 8, 12, or 18 h (4). As in our study, the nonciliated bronchiolar cell was the primary epithelial cell present after 18 h of ozone exposure in bonnet monkeys (4) due to the loss of other epithelial cells populating the respiratory bronchiole. The hypertrophy observed in nonciliated bronchiolar cells of monkey respiratory bronchioles was not unexpected since these cells respond by increasing the volume of their organelles associated with protein synthesis in a dose-dependent fashion to long-term ozone exposure (28). The marked neutrophil accumulation observed in airspaces of respiratory bronchioles at 12 and 24 h was closely correlated with neutrophils recovered by BALF. It is noteworthy that few neutrophils were observed in the epithelial compartment at 12 or 24 h by morphometry. It is also of interest that ^{111}In-labeled neutrophils showed no significant emigration into lung tissue or airspace 24 h or later after exposure. These results imply that neutrophils remain in the lung for some period of time, between 12 and 24 h after exposure. Neutrophils probably

TABLE 3

*Body weight and distribution of indium-labeled neutrophils in blood, liver, spleen, and tracheobronchial lymph nodes**

Exposure Groups	Monkeys (*n*)	Body Weight (*kg*)	Circulating % cpm 5 min	Circulating % cpm 4 h	% cpm Liver	% cpm Spleen	% cpm TB Lymph Node × 10^3
FA	5	3.40 ± 0.259	48.42 ± 2.478	15.85 ± 3.631	45.48 ± 6.932	18.11 ± 4.857	0.94 ± 0.002
8 h O_3 + 12 h FA	3	2.90 ± 0.150	42.68 ± 6.310	19.98 ± 1.951	29.79 ± 4.278	25.47 ± 7.523	1.08 ± 0.003
8 h O_3 + 24 h FA	3	3.17 ± 0.260	30.69 ± 7.904†	19.88 ± 11.928	43.91 ± 6.270	6.18 ± 2.546	2.93 ± 0.015
8 h O_3 + 72 h FA	3	2.89 ± 0.242	44.81 ± 0.185	24.48 ± 0.525	30.89 ± 13.574	7.89 ± 2.702	0.87 ± 0.013
8 h O_3 + 168 h FA	3	3.04 ± 0.190	39.83 ± 3.210	14.50 ± 5.254	49.00 ± 17.095	15.62 ± 5.889	2.86 ± 0.011

Definition of abbreviations: FA = filtered air; TB = tracheobronchial; O_3 = ozone; % cpm = percentage of total infused; cpm of ^{111}In-labeled neutrophils.
* All values are expressed as mean ± 1 SEM.
† Significantly different from ($P < 0.05$) filtered-air control.

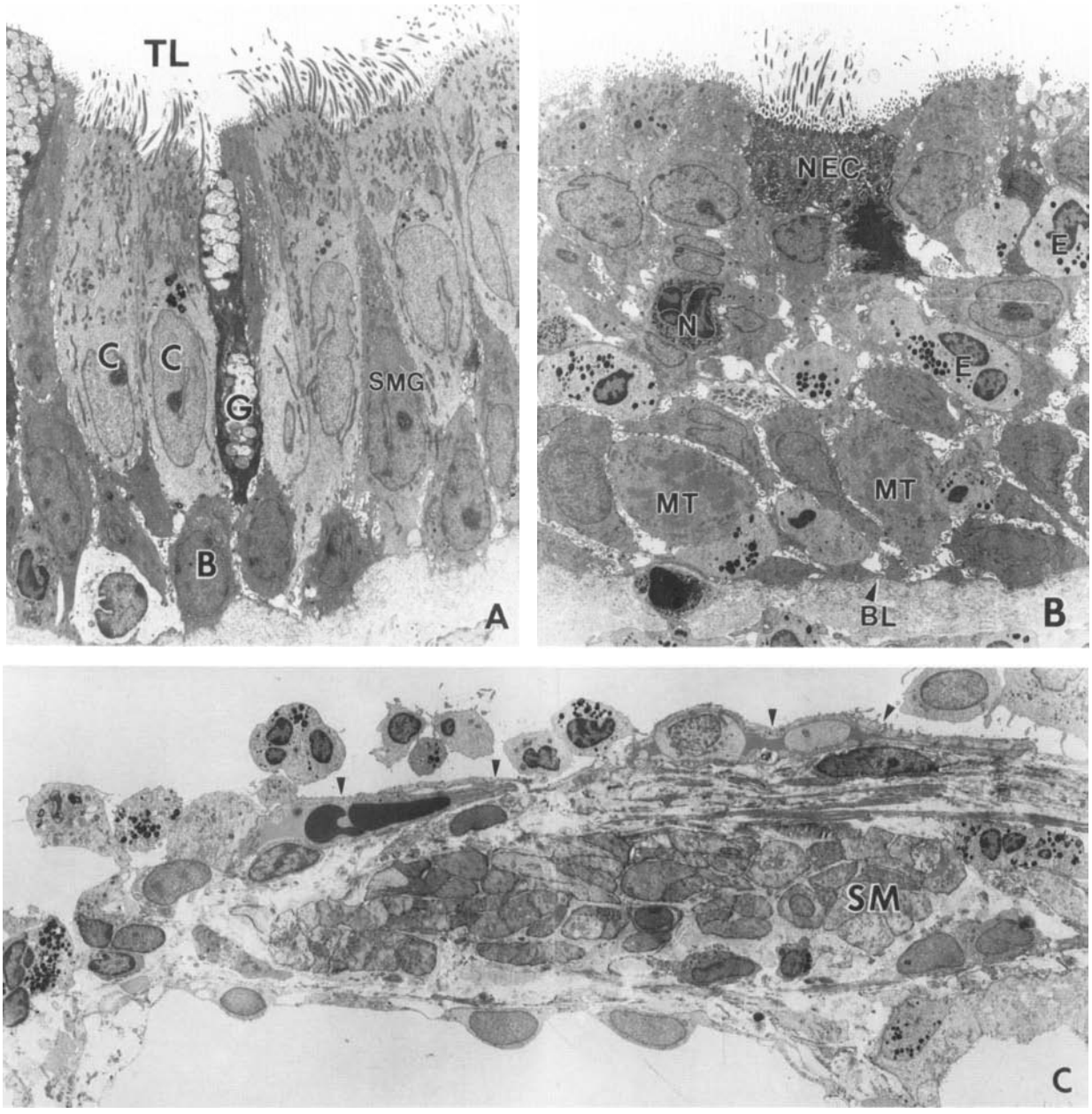

Figure 11. Airways from monkeys exposed to 8 h of 0.96 ppm ozone followed by 24 h of filtered air. *Panel A:* Trachea. Note the normal-appearing ciliated pseudostratified columnar epithelium with ciliated (C), goblet (G), small mucous granule (SMG), and basal (B) cells. TL = tracheal lumen. Magnification: ×1,863. *Panel B:* Bronchus. Note the necrotic epithelial cells at the luminal surface (NEC), neutrophils (N), eosinophils (E), and mitotic figures (MT) in the epithelium. Granulocytes are also present beneath the basal lamina (BL). Magnification: ×1,857. *Panel C:* Respiratory bronchiole. Sloughing or injured type I epithelial cells (*arrowheads*) are interspersed among undifferentiated cuboidal cells. The interstitium has a normal appearance with abundant smooth muscle (SM). The airway lumen has numerous granulocytes and mononuclear phagocytes. Magnification: ×1,622. *Panel D:* Proximal alveolar duct. Note the abundant mononuclear phagocytes (M) and neutrophils. Magnification: ×1,622.

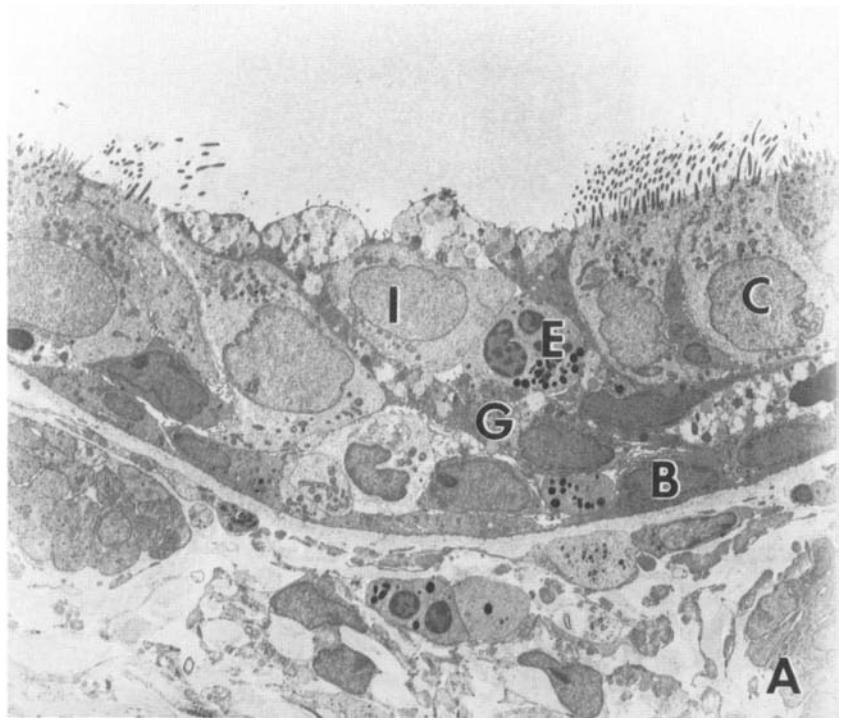

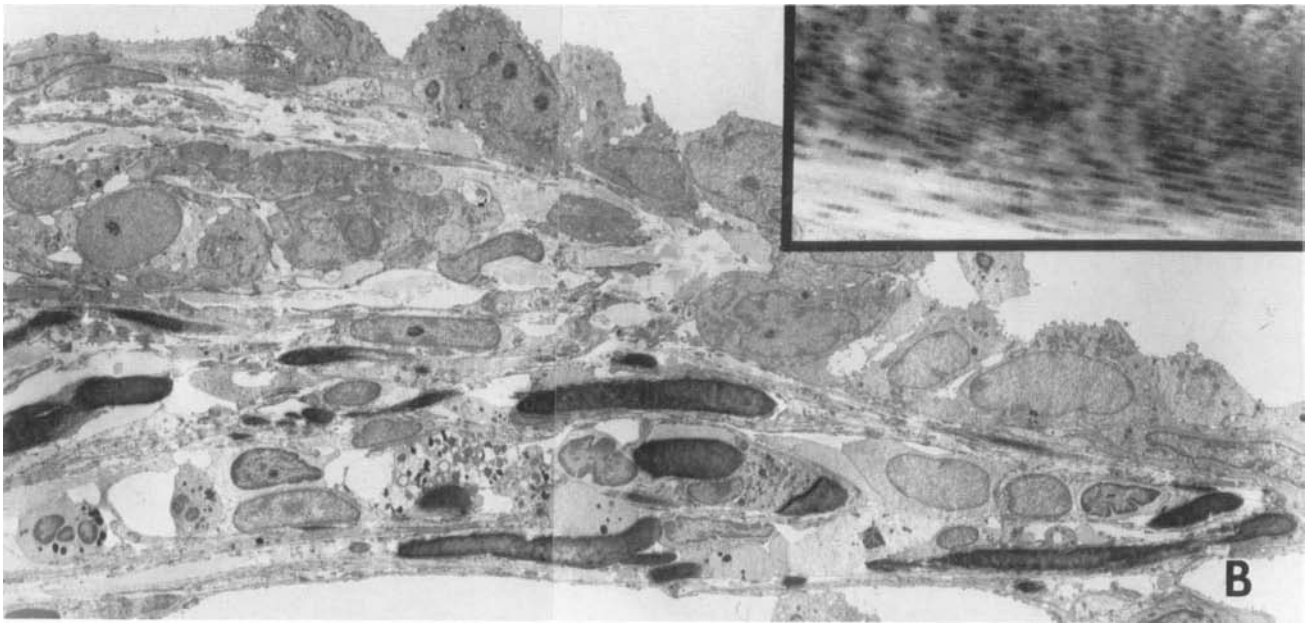

Figure 12. Airways from monkeys exposed to 8 h of 0.96 ppm ozone followed by 3 days of filtered air. *Panel A:* Bronchus. Note the eosinophils (E) in the epithelium and interstitium. The epithelium has numerous intermediate cells (I), but ciliated (C), goblet (G), and basal (B) cells are present. Magnification: ×2,068. *Panel B:* Respiratory bronchiole. Note the normal appearance of the cuboidal epithelial cells. The interstitium was marked by osmiophilic collagenous fibers (*inset*). Magnification: ×2,024; inset: ×23,760.

migrate into more proximal airways at 12 h and remain in the airways to be sampled by BALF at 24 h after exposure. Translocation of granulocytes from proximal airways to respiratory bronchioles could possibly have occurred through fixation by airway instillation.

The presence of neutrophils in the airways that were not removed between the 12- and 24-h post-exposure times was unexpected. It is possible that there was impairment of airway clearance of neutrophils, including impairment of phagocytosis of neutrophils by alveolar macrophages. Tracheobronchial clearance of inhaled insoluble radiolabeled particles in humans is minimally affected by exposure to concentrations of ozone as low as 0.2 ppm, but appears to be enhanced at higher concentrations (29). In contrast, there is decreased ability of rat alveolar macrophages to phagocytize bacteria after concentrations as low as 0.5 ppm ozone for 3 h (5). This decreased ability for phagocytosis after ozone exposure is correlated with altered alveolar macrophage membrane receptors for wheat germ agglutinin, which may be reflective of alterations in the cells' recognition capability (30). It is also possible that the normal apototic process by which neutrophils and eosinophils undergo programmed cell

TABLE 4

*Volume density of interstitial components of trachea and bronchi**

	Exposure Group†				
	FA (5)	1 h (3)	12 h (3)	24 h (3)	72 h (3)	168 h (3)
Trachea						
Smooth muscle	0.12 ± 0.12	0.11 ± 0.11	0.91 ± 0.668	1.59 ± 1.104	0.79 ± 0.594	1.91 ± 0.273
Fibroblasts	8.99 ± 0.705	9.42 ± 3.929	15.14 ± 1.453	7.58 ± 2.247	14.77 ± 1.855	13.41 ± 3.295
Amorphous matrix	55.39 ± 5.236	61.97 ± 7.735	42.56 ± 5.126	31.74 ± 9.090‡	34.15 ± 1.951	46.32 ± 3.979
Collagen fibers	25.82 ± 6.919	14.86 ± 4.766	18.29 ± 0.602	15.46 ± 4.600	25.76 ± 3.564	16.70 ± 1.127
Elastic fibers	0.15 ± 0.092	N	N	N	N	0.92 ± 0.92
Bronchi						
Smooth muscle	9.36 ± 1.613	18.08 ± 1.515	25.77 ± 7.408‡	24.59 ± 7.028‡	26.46 ± 6.983‡	30.38 ± 1.734‡
Fibroblast	12.99 ± 1.031	12.82 ± 3.453	10.64 ± 2.790	10.58 ± 2.049	9.91 ± 3.125	6.97 ± 0.304
Amorphous matrix	49.44 ± 0.778	39.05 ± 4.317	31.63 ± 3.991‡	29.20 ± 1.578‡	31.71 ± 5.526‡	18.13 ± 6.180‡
Collagen fibers	15.65 ± 0.198	21.00 ± 2.773	19.98 ± 1.789	18.21 ± 2.968	17.92 ± 4.831	8.26 ± 2.035‡
Elastic fibers	N	N	N	N	N	N

Definition of abbreviations: FA = filtered air; N = none observed.
* Data expressed as mean ± 1 SEM of percent volume density (×100) in the interstitial compartment. Number of monkeys is in parentheses.
† Groups of monkeys are based on times in filtered air after 8-h exposure to ozone. Filtered-air monkeys were only exposed to filtered air.
‡ Significantly different from ($P \leq 0.05$) filtered-air control monkeys.

death was delayed in the lung. Apotosis of neutrophils leads to their recognition and phagocytosis by macrophages (31). Elaboration of granulocyte/macrophage colony-stimulating factor (GM-CSF) by cultured human bronchial epithelial cells enhanced the survival of peripheral blood eosinophils and a neutralizing monoclonal antibody to human GM-CSF completely inhibited the increased survival of eosinophils (32). An increased survival of granulocytes and a decrease in alveolar macrophage phagocytosis could explain the retention of neutrophils in ozone-exposed monkeys.

The strongest evidence for inflammatory cell–induced injury after ozone exposure was found in bronchi. There was marked necrosis of bronchial epithelial cells and significant increases in eosinophils and neutrophils in the epithelial and interstitial compartments of these airways at 24 h after exposure. This finding was unexpected because exposure of rhesus monkeys to 0.64 ppm ozone for 3 and 7 days showed that the right mainstem bronchial epithelium was less affected than the trachea (16). It should be noted that the bronchi sampled in this study, generations 4 and 9, were much more distal. A more severe response of secretory cell metaplasia in bronchi as compared with the trachea was observed in hamsters given purified human neutrophil elastase and a crude extract of human neutrophils (33). Subsequent studies in hamsters using lectin cytochemistry showed markedly less lectin binding in bronchi as compared with trachea (34). The investigators interpreted this difference in lectin binding as a native difference in epithelial surface glycoconjugates, which may allow more human neutrophil elastase to bind on the surface of bronchial than tracheal epithelial cells. However, the issue of preferential bronchial epithelial susceptibility is probably more complex, because a dose of the crude extract of human neutrophils caused secretory cell metaplasia in bronchi of hamsters at equivalent, but ineffectual doses of purified human neutrophil elastase (33). Further, the secretory cell metaplasia induced by the crude extract of human neutrophils in hamsters was unaffected by an elastase inhibitor. Our morphometric data in monkeys exposed to ozone support the possibility that the initiation and resolution of inflammation is different in bronchi than it is

TABLE 5

*Volume of interstitial components per surface area of respiratory bronchiole epithelial basal lamina**

	Exposure Group†				
	FA (5)	1 h (3)	12 h (3)	24 h (3)	72 h (3)	168 h (3)
τ_1 (μm)‡	11.72 ± 2.026	14.58 ± 4.356	24.76 ± 5.789§	27.55 ± 2.562§	18.40 ± 0.298	16.93 ± 0.158
Smooth muscle	2.87 ± 0.598	2.27 ± 1.169	4.49 ± 0.919	6.07 ± 0.633§	2.29 ± 0.078	2.94 ± 0.039
Fibroblasts	1.66 ± 0.427	1.76 ± 0.230	2.77 ± 0.652	4.37 ± 0.431§	3.17 ± 0.057§	2.84 ± 0.040
Amorphous matrix	3.69 ± 1.145	6.08 ± 2.120	9.33 ± 2.651§	7.24 ± 0.579	6.02 ± 0.016	7.14 ± 0.036
Collagen fibers	2.52 ± 0.773	2.35 ± 0.671	3.76 ± 0.858	4.52 ± 0.909	3.51 ± 0.016	2.42 ± 0.031
Elastic fibers (× 10^2)	9.29 ± 6.667	4.29 ± 2.268	N	9.5 ± 3.209	11.77 ± 1.572	6.57 ± 1.565

Definition of abbreviations: FA = filtered air; N = none observed.
* All data expressed as mean ± 1 SEM ($\mu m^3/\mu m^2$). Number of monkeys is in parentheses.
† All groups are times after 8-h exposure to ozone, except filtered-air control in which monkeys were exposed only to filtered air.
‡ τ_1 = Arithmetic mean thickness of interstitium without small vessels, but includes inflammatory cells reported in Figure 7.
§ Significantly greater than ($P \leq 0.05$) filtered-air group.

in trachea and respiratory bronchioles. Eosinophils were much more abundant in the epithelium and interstitium of bronchi as compared with trachea and respiratory bronchioles. Eosinophil activation appears to be part of the inflammatory process in ARDS as evidenced by a significant correlation between BALF eosinophil cationic protein (ECB) and neutrophil myeloperoxidase (MPO) (35). The significant correlation between BALF ECB and MPO suggests a common activator of eosinophils and neutrophils. Eosinophil major basic protein (MBP) is found in the crystalloid core of the eosinophil granule. At a concentration of 100 μg/ml, MBP caused exfoliation of guinea pig tracheal explants (36). At lower concentrations, MBP caused ciliostasis in circumscribed areas of the tracheal epithelium. MBP inhibits active ciliated cells by direct impairment of axoneural function, probably by the inhibition of ATPase activity (37).

The observation of a decrease in secretory granules in goblet cells of the trachea and bronchi at 1 h after ozone exposure in these monkeys was in good agreement with a significant increase in mucins detected by an ELISA method in BALF supernatant. These changes in BALF mucin and goblet secretory granules were also associated with a significant increase in BALF neutrophils and the presence of neutrophils and eosinophils in airway tissue. Human neutrophil elastase, a serine protease, causes an increase in glycoconjugate release from hamster tracheal organ cultures (38). Intranasal instillation of endotoxin in rats elicits a transient influx of neutrophils into the nasal epithelium that was associated with concurrent quantitative decreases in stored epithelial mucosubstance (39). It was concluded that a transepithelial migration of neutrophils elicited a transient depletion of epithelial stored mucosubstance, because rats in which circulating neutrophils were sequestered in the lungs and prevented from migrating into endotoxin-treated nasal epithelium had no change in stored mucosubstance. Whether the change in mucous release was due to the release of secretagogues from migrating neutrophils or some other neutrophil-related method of stimulation was not determined. Mucus hypersecretion is commonly observed in bronchitis. It appears that this is a response of the epithelial cells for protection from various inflammatory agents. Mucus protects airways by creating a physical barrier between inflammatory agents and the underlying epithelium and also serves as a chemical barrier that neutralizes potentially harmful substances such as proteases (40).

Studies in another species of primates, humans, found a similar inflammatory response to our finding in rhesus monkeys. Healthy, nonsmoking male volunteers exposed to 0.4 ppm ozone for 2 h followed by 18 h in air had BAL performed and the cells and supernatant evaluated for various indicators of inflammation (41). At 18 h after exposure, there was an 8.2-fold increase in the percentage of polymorphonuclear leukocytes and a 3.8-fold increase in immunoreactive neutrophil elastase in supernatant, while its activity increased 20.6-fold in lavaged cells. The chemotactic leukotriene B_4 was unchanged whereas PGE_2 increased 2-fold, and the complement fragment C3a increased 1.7-fold. Similarly, Seltzer and co-workers (10) observed increased numbers of neutrophils and the prostaglandin products PGE_2, $PGF_{2\alpha}$, and TXB_2 in BALF of human volunteers 3 h after termination of a 2-h exposure to 0.4 or 0.6 ppm ozone. Results from monkeys exposed to ozone (0.96 ppm) for 8 h in this study showed comparable increases in neutrophils, $PGF_{2\alpha}$, PGD_2, and PGE_2 in BALF at the end of the exposure. The comparison shows that the monkey model of human ozone exposure accurately reflects the direction and general magnitude of inflammatory changes observed in BALF after voluntary human exposure.

Lung epithelial cells, alveolar macrophages, and neutrophils are a major source of arachidonic acid metabolites. There is ample evidence that these metabolites may be important mediators of the early inflammatory events seen with exposure to ozone. Exposure of rats to 1.1 ppm ozone results in a 10-fold increase in the amount of arachidonic acid recovered from the lipid of endobronchial washings (42). Increases in lavage concentrations of PGE_2 and $PGF_{2\alpha}$ were observed in rats after exposure to 4.0 ppm ozone for 2 to 8 h (43). In studies designed to further investigate the importance of prostaglandins in acute ozone lung injury, rats were treated with the prostaglandin inhibitor indomethacin prior to exposure to ozone (4 ppm, 4 h) (44). Indomethacin significantly decreased the injurious effects of ozone as determined by measured gains in lung weight as an indication of pulmonary edema. The mechanisms by which arachidonic acid metabolites mediate neutrophil-dependent injury probably involve a number of complex interactions. PGE_2 has recently been shown to increase neutrophil emigration into the lung in response to the fifth component of complement by a vasodilatory mechanism in the pulmonary microvasculature (45). The observation corresponds nicely to our observations in monkeys where the peak of PGE_2 occurred at the earliest sampling time (1 h after exposure) when neutrophils were likewise maximally increased in BALF.

Our results imply that ozone-induced epithelial necrosis is biphasic, with the early phase resulting from direct ozone injury to epithelial cells. The subsequent neutrophilic and eosinophilic response is associated in bronchi with increased epithelial necrosis and a significant increase of protein in BALF. Our results suggest that granulocytes play a critical role in acute epithelial injury resulting from ozone exposure. A critical question raised by this study is whether ozone-induced injury is time dependent in nature, with ozone-derived oxygen metabolite injury to epithelium requiring a fixed period of time before cell injury and death is evident. If this is the case, then the presence of granulocytes adjacent to injured and dying epithelial cells is just an epiphenomenon. More likely, the true case is some combination from both sources of injury. The present study more clearly defines the relationship between granulocyte activity and epithelial injury in acute ozone exposure that allows the design of experiments to better define the contribution of each method of injury. Understanding the linkage between ozone-induced acute epithelial injury and later manifestations of pulmonary disease will have an important bearing on elucidating the pathogenesis of small airway or centriacinar disease caused by a variety of inhaled irritants, including cigarette smoke.

Acknowledgments: The writers thank Mary Stovall for her technical assistance. This work was supported by Grant ES-00628 from the National Institute of Environmental Health Sciences.

References

1. Williams, S. J., J. M. Charles, and D. B. Menzel. 1980. Ozone induced alterations in phenol red absorption from the rat lung. *Toxicol Lett.* 6:213–219.
2. Aranyi, C., S. C. Vana, P. T. Thomas, J. N. Bradof, and J. D. Fenters. 1983. Effects of subchronic exposure to a mixture of O_3, SO_2, and $(NH_4)_2SO_4$ on host defenses of mice. *J. Toxicol. Environ. Health* 12: 55–71.
3. Stephens, R. J., M. F. Sloan, M. J. Evans, and G. Freeman. 1973. Early response of lung to low levels of ozone. *Am. J. Pathol.* 74:31–58.
4. Castleman, W. L., D. L. Dungworth, L. W. Schwartz, and W. S. Tyler. 1980. Acute respiratory bronchiolitis: an ultrastructural and autoradiographic study of epithelial cell injury and renewal in rhesus monkeys exposed to ozone. *Am. J. Pathol.* 98:811–840.
5. Coffin, D., D. E. Gardner, R. S. Holzman, and F. J. Wolock. 1968. Influence of ozone on pulmonary cells. *Arch. Environ. Health* 16:633–636.
6. Bassett, D. J. P., E. Bowen-Kelly, E. L. Brewster *et al.* 1988. A reversible model of acute lung injury based on ozone exposure. *Lung* 166:355–369.
7. Shasby, D. M., R. B. Fox, R. N. Harada, and J. E. Repine. 1982. Reduction of the edema of acute hyperoxic lung injury by granulocyte depletion. *J. Appl. Physiol.* 52:1237–1244.
8. Schraufstatter, I. U., S. D. Revak, and C. G. Cochrane. 1984. Proteases and oxidants in experimental pulmonary inflammatory injury. *J. Clin. Invest.* 73:1175–1184.
9. Hogg, J. C. 1987. Neutrophil kinetics and lung injury. *Physiol. Rev.* 67:1249–1295.
10. Seltzer, J., B. G. Bigby, M. Stulbarg *et al.* 1986. O_3-induced change in bronchial reactivity to methacholine and airway inflammation in humans. *J. Appl. Physiol.* 60:1321–1326.
11. Hinners, R. G., J. K. Burkart, and C. L. Punte. 1968. Animal inhalation exposure chambers. *Arch. Environ. Health* 16:194–206.
12. Haslett, C., L. A. Guthrie, M. M. Kopaniak, R. B. Johnston, Jr., and P. M. Henson. 1985. Modulation of multiple neutrophil functions by preparative methods or trace concentrations of bacterial lipopolysaccharide. *Am. J. Pathol.* 119:101–110.
13. Lowry, O. H., N. J. Rosebrough, A. L. Farr, and R. J. Randall. 1951. Protein measurement with the folin phenol reagent. *J. Biol. Chem.* 193:265–275.
14. Plopper, C. G., A. T. Mariassy, and L. O. Lollini. 1984. Structure as revealed by airway dissection. A comparison of mammalian lungs. *Am. Rev. Respir. Dis.* 128:54–57.
15. Cruz-Orive, L. M., and E. R. Weibel. 1981. Sampling designs for stereology. *J. Microsc.* 122:235–257.
16. Wilson, D. W., C. G. Plopper, and D. L. Dungworth. 1984. The response of the macaque tracheobronchial epithelium to acute ozone injury. *Am. J. Pathol.* 116:193–206.
17. Weibel, E. R. 1979. Stereological Methods. Academic Press, London.
18. Baddeley, A. J., H. J. G. Gundersen, and L. M. Cruz-Orive. 1986. Estimation of surface area from vertical sections. *J. Microsc.* 142:259–276.
19. Liu, M. C., E. R. Bleecker, D. Proud, T. L. McLemore, and W. C. Hubbard. 1988. Profiling of bisenoic prostaglandins and thromboxane B_2 in bronchoalveolar fluid from the lower respiratory tract of human subjects by combined capillary gas chromatography-mass spectrometry. *Prostaglandins* 35:69–81.
20. Lin, H., D. M. Carlson, J. A. St. George, C. G. Plopper, and R. Wu. 1989. An ELISA method for the quantitation of tracheal mucins from human and nonhuman primates. *Am. J. Respir. Cell Mol. Biol.* 1:41–48.
21. SAS Institute. 1985. SAS/STAT guide for personal computers, version 6. SAS Institute, Cary, NC.
22. Gerrity, T. R., W. A. Weaver, J. Berntsen, D. E. House, and J. J. O'Neil. 1988. Extrathoracic and intrathoracic removal of O_3 in tidal-breathing humans. *J. Appl. Physiol.* 65:393–400.
23. Cochrane, C. G., R. G. Spragg, and S. D. Revak. 1983. Studies on the pathogenesis of the adult respiratory distress syndrome: evidence of oxidant activity in bronchoalveolar lavage fluid. *J. Clin. Invest.* 71:754–761.
24. Lee, C. T., A. M. Fein, M. Lippmann, H. Holtzman, P. Kimbel, and G. Weinbaum. 1981. Elastolytic activity in pulmonary lavage fluid from patients with adult respiratory distress syndrome. *N. Engl. J. Med.* 304: 192–196.
25. Zhu, Q., A. V. Singh, A. Bateman, F. Esch, and S. Solomon. 1987. The corticostatic (anti-ACTH) and cytotoxic activity of peptides isolated from fetal, adult and tumor-bearing lung. *J. Steroid Biochem.* 27:1017–1022.
26. Zhu, Q., H. Jing, S. Mulay, F. Esch, S. Shimasaki, and S. Solomon. 1988. Isolation and structure of corticostatin peptides from rabbit fetal and adult lung. *Proc. Natl. Acad. Sci. USA* 85:592–596.
27. Lehrer, R. I., and T. Ganz. 1990. Antimicrobial polypeptides of human neutrophils. *Blood* 76:2169–2181.
28. Moffatt, R. K., D. M. Hyde, C. G. Plopper, W. S. Tyler, and L. F. Putney. 1987. Ozone-induced adaptive and reactive cellular changes in respiratory bronchioles of bonnet monkeys. *Exp. Lung Res.* 12:57–74.
29. Foster, W. M., D. L. Costa, and E. G. Langenback. 1987. Ozone exposure alters tracheobronchial mucociliary function in humans. *J. Appl. Physiol.* 63:996–1002.
30. Hadley, J. G., D. E. Gardner, D. L. Coffin, and D. B. Menzel. 1977. Enhanced binding of autologous cells to the macrophage plasma membrane as a sensitive indicator of pollutant damage. *In* Pulmonary Macrophage and Epithelial Cells: Proceedings of the Sixteenth Annual Hanford Biology Symposium; September 1976, Richland, WA. C. L. Sanders, R. P. Schneider, G. E. Dagle, and H. A. Ragan, editors. Energy Research and Development Administration, Washington, DC. (ERDA symposium series: vol. 43.) Available from: NTIS, Springfield, VA; CONF-760927.
31. Savill, J. S., A. H. Wyllie, J. E. Henson, M. J. Walport, P. M. Henson, and C. Haslett. 1989. Macrophage phagocytosis of aging neutrophils in inflammation. Programmed cell death in the neutrophil leads to its recognition by macrophages. *J. Clin. Invest.* 83:865–875.
32. Cox, G., T. Ohtoshi, C. Vancheri *et al.* 1991. Promotion of eosinophil survival by human bronchial epithelial cells and its modulation by steroids. *Am. J. Respir. Cell Mol. Biol.* 4:525–531.
33. Snider, G. L., E. C. Lucey, T. G. Christensen *et al.* 1984. Emphysema and bronchial secretory cell metaplasia induced in hamsters by human neutrophil products. *Am. Rev. Respir. Dis.* 129:155–160.
34. Christensen, T. B., R. Breuer, E. C. Lucey, L. J. Hornstra, P. J. Stone, and G. L. Snider. 1990. Lectin cytochemistry reveals differences between hamster trachea and bronchus in the composition of epithelial surface glycoconjugates and in the response of secretory cells to neutrophil elastase. *Am. J. Respir. Cell Mol. Biol.* 3:61–69.
35. Hallgren, R., T. Samuelsson, P. Venge, and J. Modig. 1987. Eosinophil activation in the lung is related to lung damage in respiratory distress syndrome. *Am. Rev. Respir. Dis.* 135:639–642.
36. Frigas, E., D. A. Loegering, and G. J. Gleich. 1980. Cytotoxic effects of the guinea pig eosinophil major basic protein on tracheal epithelium. *Lab. Invest.* 42:35–43.
37. Hastie, A. T., D. A. Loegering, G. J. Gleich, and F. Kueppers. 1987. The effect of purified human eosinophil major basic protein on mammalian ciliary activity. *Am. Rev. Respir. Dis.* 135:848–853.
38. Niles, R. M., T. G. Christensen, B. Raphel, P. J. Stone, and G. L. Snider. 1986. Serine proteases stimulate mucous glycoprotein release from hamster tracheal ring organ culture. *J. Lab. Clin. Med.* 108:489–497.
39. Harkema, J. R., J. A. Hotchkiss, A. G. Harmsen, and R. F. Henderson. 1988. *In vivo* effects of transient neutrophil influx on nasal respiratory epithelial mucosubstances. Quantitative histochemistry. *Am. J. Pathol.* 130: 605–615.
40. Kaliner, M., J. H. Shelhamer, B. Borson, J. Nadel, C. Patow, and Z. Marow. 1986. Human respiratory mucus. *Am. Rev. Respir. Dis.* 134: 612–621.
41. Koren, H. S., R. B. Devlin, D. E. Graham *et al.* 1989. Ozone-induced inflammation in the lower airways of human subjects. *Am. Rev. Respir. Dis.* 139:407–415.
42. Shimasaki, H., T. Takatori, W. R. Anderson, H. L. Horten, and O. S. Privett. 1976. Alteration of lung lipids in ozone exposed rats. *Biochem. Biophys. Res. Commun.* 68:1256–1262.
43. Giri, S. N., M. A. Hollinger, and M. J. Schiedt. 1980. The effects of ozone and paraquat on $PGF_{2\alpha}$ and PGE_2 levels in plasma and combined pleural effusion and lung lavage of rats. *Environ. Res.* 21:467–476.
44. Giri, S. N., J. Benson, D. M. Siegel, S. A. Rice, and M. Schiedt. 1975. Effects of pretreatment with anti-inflammatory drugs on ozone-induced lung damage in rats. *Proc. Soc. Exp. Biol. Med.* 150:810–814.
45. Downey, G. P., R. S. Gumbay, G. S. Worthen, D. E. Doherty, J. E. Henson, and P. M. Henson. 1988. Enhancement of pulmonary inflammation by prostaglandin E: evidence for a vasodilator effect. *J. Appl. Physiol.* 64:728–741.